AGU PUBLICATIONS

Geophysical Research Letters

RESEARCH LETTER
10.1002/2014GL061399

Key Points:
- We developed and assessed five microbial enzyme models against field data
- DOC accumulates in dry soil pore and is available to microbe in response to rain
- The transitions of DOC and enzymes between dry and wet soil pores are important

Correspondence to:
G.-Y. Niu,
niug@email.arizona.edu

Citation:
Zhang, X., G.-Y. Niu, A. S. Elshall, M. Ye, G. A. Barron-Gafford, and M. Pavao-Zuckerman (2014), Assessing five evolving microbial enzyme models against field measurements from a semiarid savannah—What are the mechanisms of soil respiration pulses?, *Geophys. Res. Lett.*, *41*, 6428–6434, doi:10.1002/2014GL061399.

Received 31 JUL 2014
Accepted 6 SEP 2014
Accepted article online 11 SEP 2014
Published online 25 SEP 2014

Assessing five evolving microbial enzyme models against field measurements from a semiarid savannah—What are the mechanisms of soil respiration pulses?

Xia Zhang[1,2], Guo-Yue Niu[2,3], Ahmed S. Elshall[4], Ming Ye[4], Greg A. Barron-Gafford[2,5], and Mitch Pavao-Zuckerman[2,6]

[1]Key Laboratory of Regional Climate-Environment Research for Temperate East Asia, Institute of Atmospheric Physics, Chinese Academy of Sciences, Beijing, China, [2]Biosphere 2, University of Arizona, Tucson, Arizona, USA, [3]Department of Hydrology and Water Resources, University of Arizona, Tucson, Arizona, USA, [4]Department of Scientific Computing, Florida State University, Tallahassee, Florida, USA, [5]School of Geography and Development, University of Arizona, Tucson, Arizona, USA, [6]School of Natural Resources and Environment, University of Arizona, Tucson, Arizona, USA

Abstract Soil microbial respiration pulses in response to episodic rainfall pulses (the "Birch effect") are poorly understood. We developed and assessed five evolving microbial enzyme models against field measurements from a semiarid savannah characterized by pulsed precipitation to understand the mechanisms to generate the Birch pulses. The five models evolve from an existing four-carbon (C) pool model to models with additional C pools and explicit representations of soil moisture controls on C degradation and microbial uptake rates. Assessing the models using techniques of model selection and model averaging suggests that models with additional C pools for accumulation of degraded C in the dry zone of the soil pore space result in a higher probability of reproducing the observed Birch pulses. Degraded C accumulated in dry soil pores during dry periods becomes immediately accessible to microbes in response to rainstorms, providing a major mechanism to generate respiration pulses. Explicitly representing the transition of degraded C and enzymes between dry and wet soil pores in response to soil moisture changes and soil moisture controls on C degradation and microbial uptake rates improve the models' efficiency and robustness in simulating the Birch effect. Assuming that enzymes in the dry soil pores facilitate degradation of complex C during dry periods (though at a lower rate) results in a greater accumulation of degraded C and thus further improves the models' performance. However, the actual mechanism inducing the greater accumulation of labile C needs further experimental studies.

1. Introduction

Global soils store 2300 Pg carbon (C), an amount more than 3 times that of the atmosphere [*Schmidt et al.*, 2011] and release 60–75 Pg C/yr, about 10 times more CO_2 to the atmosphere than all human-caused emissions [*Schlesinger and Andrews*, 2000]. Coupled C-climate models projected a high variability in global soil C storage [*Todd-Brown et al.*, 2013], atmospheric CO_2 concentration, and hence various rates of warming [*Friedlingstein et al.*, 2006]. Recognizing the flaws of the first-order decay kinetics currently used in most coupled C-climate models, researchers have developed new soil organic carbon (SOC) decomposition models to directly link SOC turnover to microbial growth and physiology [*Schimel and Weintraub*, 2003; *Allison et al.*, 2010; *Wieder et al.*, 2013].

Microbes produce extracellular enzymes to degrade complex SOC into dissolved organic C (DOC) through catalysis and assimilate DOC into microbial biomass for growth, releasing CO_2 during respiration [*Sinsabaugh et al.*, 1991]. Moreover, microbial communities may change in biomass, shift in composition, or adapt physiologically in response to changes in environmental conditions, and thus mediate SOC decomposition [*Luo et al.*, 2001; *Schimel et al.*, 2007; *Bradford et al.*, 2008; *Frey et al.*, 2013]. These fundamental processes have been represented in recent microbial enzyme models [*Schimel and Weintraub*, 2003; *Allison et al.*, 2010] by implementing the Dual Arrhenius and Michaelis-Menten kinetics (DAMM) [*Davidson et al.*, 2012] and the concept of microbial C use efficiency (CUE) [*Allison et al.*, 2010; *Wieder et al.*, 2013]. The Arrhenius kinetics represents increases in decomposition with temperature and dependence on substrate quality through activation energy, while the Michaelis-Menten kinetics represents the limitation of substrate

©2014. American Geophysical Union. All Rights Reserved.

Table 1. Model Formulations of the SOC Degradation and Microbial Uptake Rates[a]

Models	Formulations
4C_NOSM	$V_{\text{decom}} = f_d(C_{\text{ENZ}}) = V_{\max} C_{\text{ENZ}} \frac{C_{\text{SOC}}}{K_m + C_{\text{SOC}}}$; $V_{\text{uptake}} = f_u(C_{\text{DOC}}) = V_{\max\_\text{up}} C_{\text{MIC}} \frac{C_{\text{DOC}}}{K_{m\_\text{up}} + C_{\text{DOC}}} \frac{C_{\text{O2}}}{K_{m\_\text{upO2}} + C_{\text{O2}}}$
4C	$V_{\text{decom}} = f_d(C_{\text{ENZ}})(\theta/\theta_s)$; $V_{\text{uptake}} = f_u(C_{\text{DOC}})(\theta/\theta_s)$
5C_NOSM	$V_{\text{decom}} = f_d(C_{\text{ENZ}})$; $V_{\text{uptake}} = f_u(C_{\text{DOC\_}W})$
5C	$V_{\text{decom}} = f_d(C_{\text{ENZ}})(\theta/\theta_s)$; $V_{\text{uptake}} = f_u(C_{\text{DOC\_}W})(\theta/\theta_s)$
6C	$V_{\text{decom\_}W} = f_d(C_{\text{ENZ\_}W})(\theta/\theta_s)$; $V_{\text{decom\_}D} = f_d(C_{\text{ENZ\_}D})(1-\theta/\theta_s)\varepsilon_D$; $V_{\text{uptake}} = f_u(C_{\text{DOC\_}W})(\theta/\theta_s)$

[a]Where V_{decom} is SOC degradation rate; V_{uptake} microbial uptake rate; C_{SOC} SOC pool size (g C m^{-3}); C_{DOC} DOC pool size (g C m^{-3}); C_{MIC} microbial biomass pool size (g C m^{-3}); C_{ENZ} enzyme pool size (g C m^{-3}); C_{O2} (m^3 m^{-3}) the gas concentration of O_2 in the soil pore; $V_{\max}$ (s^{-1}) the maximum SOC degradation rate per unit enzyme when substrates are not limiting; K_m the half-saturation constant for SOC; $V_{\max\_\text{up}}$ the maximum DOC uptake rate (s^{-1}) when substrates are not limiting; K_{m_up} (g C m^{-3}) and K_{m_upO2} (m^3 m^{-3}) are the corresponding half saturation constants for DOC and O_2, respectively; $V_{\text{decom\_}W}$ and $V_{\text{decom\_}D}$ are the SOC degradation rates in the wet and dry zones, respectively; $C_{\text{DOC\_}W}$ (g C m^{-3}) DOC pool size in the wet soil pores; $C_{\text{DOC\_}D}$ (g C m^{-3}) degraded C (dissolvable but not dissolved) pool size in the dry soil pores; $C_{\text{ENZ\_}W}$ (g C m^{-3}) and $C_{\text{ENZ\_}D}$ (g C m^{-3}) are the enzyme pool sizes in the wet and dry soil pores; θ is volumetric soil moisture; θ_s porosity; and ε_D is the catalysis efficiency of the dry zone enzymes. Readers can refer to *Allison et al.* [2010] for formulations of $V_{\max}$, $V_{\max\_\text{up}}$, K_m, and K_{m_up}, as functions of temperature, and *Davidson et al.* [2012] for K_{m_upO2} as a constant.

availability (C and O_2) and chemical affinity of substrates on temperature sensitivity [*Davidson and Janssens*, 2006]. In addition, these models represent the temperature sensitivity using microbial CUE, which controls microbial growth, enzyme production, and microbial respiration [*Allison et al.*, 2010; *Bradford et al.*, 2008; *Frey et al.*, 2013; *Manzoni et al.*, 2012]. A small change in CUE may have profound effects on soil CO_2 production and soil C dynamics [*Allison et al.*, 2010; *Wieder et al.*, 2013].

Microbes typically operate in the wet pores of the soil pore space, and hence, their activity is largely affected by soil moisture. Soil moisture controls the transport of substrates (e.g., O_2 and DOC) and thus regulates microbial accessibility to these substrates. During dry periods, low soil water content decreases diffusion and advection of solutes, thereby limiting the supply of substrates to microbial communities and reducing microbial biomass growth and soil respiration rates [*Skopp et al.*, 1990; *Moyano et al.*, 2013]. The transient effects of soil moisture on soil respiration have long been observed from laboratory and field experiments. Pulsed wetting causes a dramatic increase in soil respiration after a period of drought (known as the "Birch effect" [*Birch*, 1958]), sustaining greater microbial biomass than constantly moist soils and resulting in greater CO_2 efflux [*Moyano et al.*, 2013; *Jarvis et al.*, 2007; *Miller et al.*, 2005]. Various mechanisms causing the Birch effect have been proposed such as sudden release of osmoregulatory substances accumulated at low water potentials, extracellular enzyme activities unaffected by soil moisture, spontaneous increase in microbial biomass in response to wetting, increase in dead microbial biomass caused by drying, microbial cell lysis, photodegradation, and destruction of soil aggregates [*Lawrence et al.*, 2009; *Schimel et al.*, 2007; *Moyano et al.*, 2013; *Jarvis et al.*, 2007; *Miller et al.*, 2005]. Due to a lack of understanding of the exact mechanism underlying the Birch effect, conventional first-order decay models represent soil moisture controls on microbial respiration in a variety of ways, such as linear or nonlinear functions of soil water content or water potential as summarized in *Reichstein and Beer* [2008]. *Lawrence et al.* [2009] suggested that within a microbial enzyme model framework, accumulation of labile C during dry periods provides a promising mechanism to reproduce respiration pulses measured during periodic rewetting experiments in laboratory. Adopting this concept, we developed five evolving microbial enzyme models with different numbers of C pools in separated dry and wet soil pores and with (or without) explicit representations of soil moisture controls on SOC degradation and microbial uptake rates to explore the mechanisms that generate the Birch pulses. We then assessed these models against field measurements from a semiarid savannah ecosystem driven by episodic rainfall pulses.

2. Methods

2.1. Models

Table 1 lists the formulations of SOC degradation and microbial uptake rates of the five models. We started with a model of *Allison et al.* [2010] that includes four C pools of SOC, DOC, microbial biomass (MIC), and enzymes (ENZ) but without an explicit representation of soil moisture controls on the rates or O_2 limitation

©2014. American Geophysical Union. All Rights Reserved.

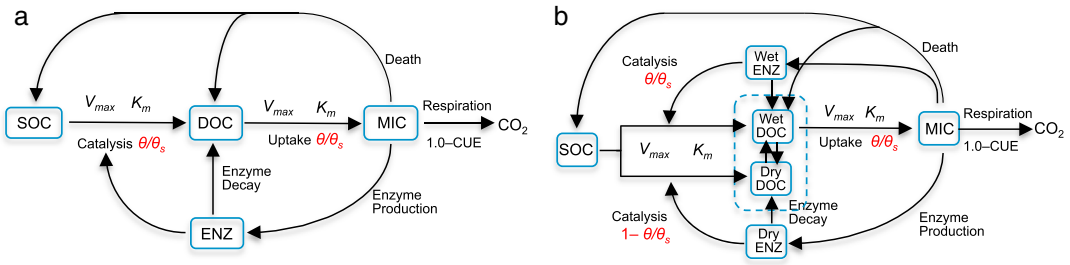

Figure 1. Diagrams of the (a) 4C and (b) 6C models. The 4C model represents processes of degradation of SOC into DOC through catalysis of enzymes (ENZ) produced by microbes (MIC) and microbial uptake of DOC and respiration. SOC degradation and microbial uptake rates are controlled by water saturation (θ/θ_s). The 6C pool model splits DOC and ENZ pools into two subpools, respectively, one for the wet zone and the other for the dry zone of the soil pore space. Microbial uptake of DOC occurs only in the wet zone, and the uptake rate is linearly related to θ/θ_s. Catalysis through ENZ in the wet zone is proportional to θ/θ_s, while that in the dry zone is proportional to $1-\theta/\theta_s$ at a reduced efficiency.

(4C_NOSM in Table 1). Following *Davidson et al.*'s [2012] model, we added O_2 limitation to all the five models. The second model (4C in Table 1 and Figure 1a) is the same as 4C_NOSM, but the rates are revised with soil moisture controls. The third model (5C_NOSM) splits DOC into two subpools, one for the wet zone and the other for the dry zone of the soil pores; however, the rates are not controlled by soil moisture. In this model, microbes can only access DOC in the wet pores. DOC in the dry pores (dissolvable but not dissolved) is the residual DOC that is not consumed by microbes and thus remained in the dry soil pores (due to contraction of hydroscopic film); it is controlled only by changes in the volume of dry and wet pores without any additional production inputs through SOC degradation. The fourth model (5C in Table 1) is the same as 5C_NOSM, but the rates are revised with soil moisture controls. The fifth model (6C in Table 1) splits both DOC and ENZ into two subpools for the wet and dry pores and allows mass changes corresponding to changes in soil water volume (Figure 1b). This model allows additional SOC degradation in the dry pores through catalysis of ENZ in the dry pores but at a reduced efficiency due to enzyme immobilization [*Alster et al.*, 2013]. Generally, enzymes in the dry pores have a lower turnover rate due to protection from degradation [*Alster et al.*, 2013].

We simply use a linear relationship between the rates and soil moisture (in degree of water saturation; see Table 1), although other forms of the relationship exist [*Lawrence et al.*, 2009; *Davidson et al.*, 2012]. At both very low and at high water contents, the relationship is likely to be nonlinear [*Moyano et al.*, 2013]. For instance, as soil moisture approaches saturation, O_2 concentration decreases and becomes a limiting factor for the microbial aerobic activities; at very low water content, diffusion through very thin and discontinuous water films is highly limiting. However, a mechanistic representation of the soil moisture effects on the supply of substrates through an explicit representation of transport of these substrates through soil water at pore scales is beyond the scope of this paper. For the majority of the range of soils moisture experienced at this study site, we assume that an empirical linear relationship is adequate.

We developed a scheme for the transition of DOC between the wet and dry zones. When soil moisture increases, the transition of degraded C from the dry to the wet pores is a portion of the degraded C in the dry pores (C_{DOC_D}) that is wetted within a time step: $F_{VW}\, C_{DOC\_D}$. $F_{VW} = (\theta^N - \theta^{N-1})/(\theta_S - \theta^{N-1})$ is the wetted fraction (relative to previous dry volume), where θ^N and θ^{N-1} are volumetric water content at current (N) and previous ($N-1$) time steps, respectively, and θ_s is porosity dependent on soil texture. When soil moisture decreases, the transition of DOC from the wet to the dry pores is a portion of the degraded C in the wet pores (C_{DOC_W}) that is dried within a time step: $F_{VD}C_{DOC\_W}$. $F_{VD} = (\theta^{N-1} - \theta^N)/\theta^{N-1}$ is the dried fraction (relative to previous wet volume). This mass-conservative scheme is also implemented for the transition of enzymes in model 6C.

2.2. Observational Data

The study site is located within the Santa Rita Experimental Range (SRER, 31.8214°N, 110.8661°W, elevation 1116 m) outside of Tucson, Arizona [*Scott et al.*, 2009; *Barron-Gafford et al.*, 2011]. This savannah site was covered by 22% perennial grass, forbs and subshrubs, and 35% of mesquite. The soils are uniformly Comoro loamy sand (77.6% sand, 11.0% clay, and 11.4% silt). The half-hourly atmospheric forcing data to drive the models were collected from measurements through an eddy covariance tower [*Scott et al.*, 2009]. Volumetric CO_2 concentration was measured at half-hourly interval through compact probes. CO_2 efflux was derived

©2014. American Geophysical Union. All Rights Reserved.

Table 2. Root-Mean-Square-Error (RMSE) and ΔBIC, Given the Best Realization[a]

Model	RMSE (μmol m^{-2} s^{-1})	ΔBIC	Model Probability [−]	Model Efficiency ε [−]
4C_NOSM	0.712	14,454	0.11	$0.47 \pm 9 \times 10^{-5}$
4C	0.664	12,332	0.16	$0.54 \pm 9 \times 10^{-5}$
5C_NOSM	0.570	7,656	0.19	$0.66 \pm 7 \times 10^{-5}$
5C	0.528	5,358	0.25	$0.71 \pm 5 \times 10^{-5}$
6C	0.443	0	0.29	$0.80 \pm 4 \times 10^{-5}$

[a]Model probability and model efficiency ε (mean ± standard deviation), given the MCMC ensemble.

from the gradient of CO_2 concentration measured at two depths of 2 cm and 10 cm through Fick's first law of diffusion and validated against measurements from a portable CO_2 gas analyzer. The half-hourly volumetric soil moisture was measured using commercial soil moisture probes at eight depths of 5, 10, 20, 30, 50, 70, 100, and 130 cm. The data used in this study are during the whole year of 2007 covering a long period of dry season prior to the monsoon and episodic rainfall events during the monsoon season.

2.3. Model Evaluation and Parameter Estimation

We use the observed soil moisture and temperature at 10 cm to drive the five microbial enzyme models. We use the community NoahMP land surface model [*Niu et al*., 2011], which includes a dynamic vegetation model, to produce root exudates and leaf litter as inputs to the soil C pool of the five models. We added the NoahMP-produced autotrophic root respiration to the total soil CO_2 efflux for comparing with the observed. We set up soil C initial values according to total C concentration measured in SRER [*McClaran et al*., 2008] for the top 43.2 cm soil.

Considering the uncertainties in model parameters, we estimate the base CUE ε_0 (g/g), enzyme production rate k_e (g/m^3 s), microbial turnover rate τ_m (1/s), and enzyme turnover rate τ_e (1/s) over a wide prior parameter space of 0.2–0.95, 1×10^{-12}–1×10^{-6}, 1×10^{-11}–1×10^{-6}, and 1×10^{-12}–1×10^{-7}, respectively. Other parameters, whose values are from *Allison et al*. [2010], are fixed. Two extra parameters in the 6C model, which are the catalysis efficiency ε_D [−] and turnover rate of the dry zone enzymes τ_{ed} [1/s] are also estimated with the prior range of 0.2–0.8 and 1×10^{-12}–1×10^{-8}, respectively. We estimate the posterior probability density function of the unknown parameters and the CO_2 efflux simulations using the Markov chain Monte Carlo (MCMC) MT-DREAM$_{(ZS)}$ sampler [*Laloy and Vrugt*, 2012] with the Gaussian likelihood function. For each model, 4×10^5 samples are drawn using four Markov chains. Although the *Gelman and Rubin* [1992] R statistic for convergence diagnostic approaches one in less than 1×10^4 sample period, the initial 50% samples are discarded during the burn-in period.

We comparatively evaluate the simulations of the five models using three assessment criteria, which are Bayesian information criterion (BIC), model probability, and Nash-Sutcliffe model efficiency, ε. BIC is a commonly used model selection criterion to select the best model from a model set with consideration of goodness of fit and model complexity. When selecting a single model cannot be justified by available data and knowledge, model probability is used to measure plausibility of a model relative to other models. ε is commonly used to measure performance of a model for different parameter sets. Following equation (3) of *Ye et al*. [2008], we computed $\mathrm{BIC} = -2\ln(\hat{L}) + k\ln(n)$, where n is the number of observations ($n = 15{,}272$), k the number of free parameters (six in the 6C model while four in the other models), and $\hat{L}$ the maximum likelihood of the MCMC sample. The second term of BIC represents a penalty for k. A model with a lower BIC is preferable. Table 2 shows the $\Delta\mathrm{BIC} = \mathrm{BIC} - \mathrm{BIC}_{\min}$, where $\mathrm{BIC}_{\min}$ is the minimum BIC value among all the models. (The best realization of model 6C has the minimum BIC; $\mathrm{BIC}_{\min} = -24{,}810$.) With uniform prior model probability, the model probability is evaluated as $P(M_i|D) = P(D|M_i)/\sum_{i=1}^{5} P(D|M_i)$, which is the ratio of the marginal likelihood $P(D|M_i)$ of the respective models M_i given observational data D. Following equation (11) of *Kass and Raftery* [1995], we estimate the marginal likelihoods $P(D|M_i) = \left\{ {}^{1}\!/\!_{N} \sum_{n=1}^{N} P(D|\theta_n, M_i)^{-1} \right\}^{-1}$ by taking the geometric mean of the joint likelihoods $P(D|\theta_n, M_i)$ of the parameter samples θ_n and model M_i, using MCMC ensemble of $N = 2 \times 10^5$ samples after discarding the burn-in samples. The estimated model probabilities are listed in Table 2. Models are ranked according to their model probabilities such that the best model and the worst model have the highest and lowest posterior model probabilities, respectively. The third assessment criterion is ε, which is a measure of model robustness in capturing the observed variability (especially sensitive to peak values).

©2014. American Geophysical Union. All Rights Reserved.

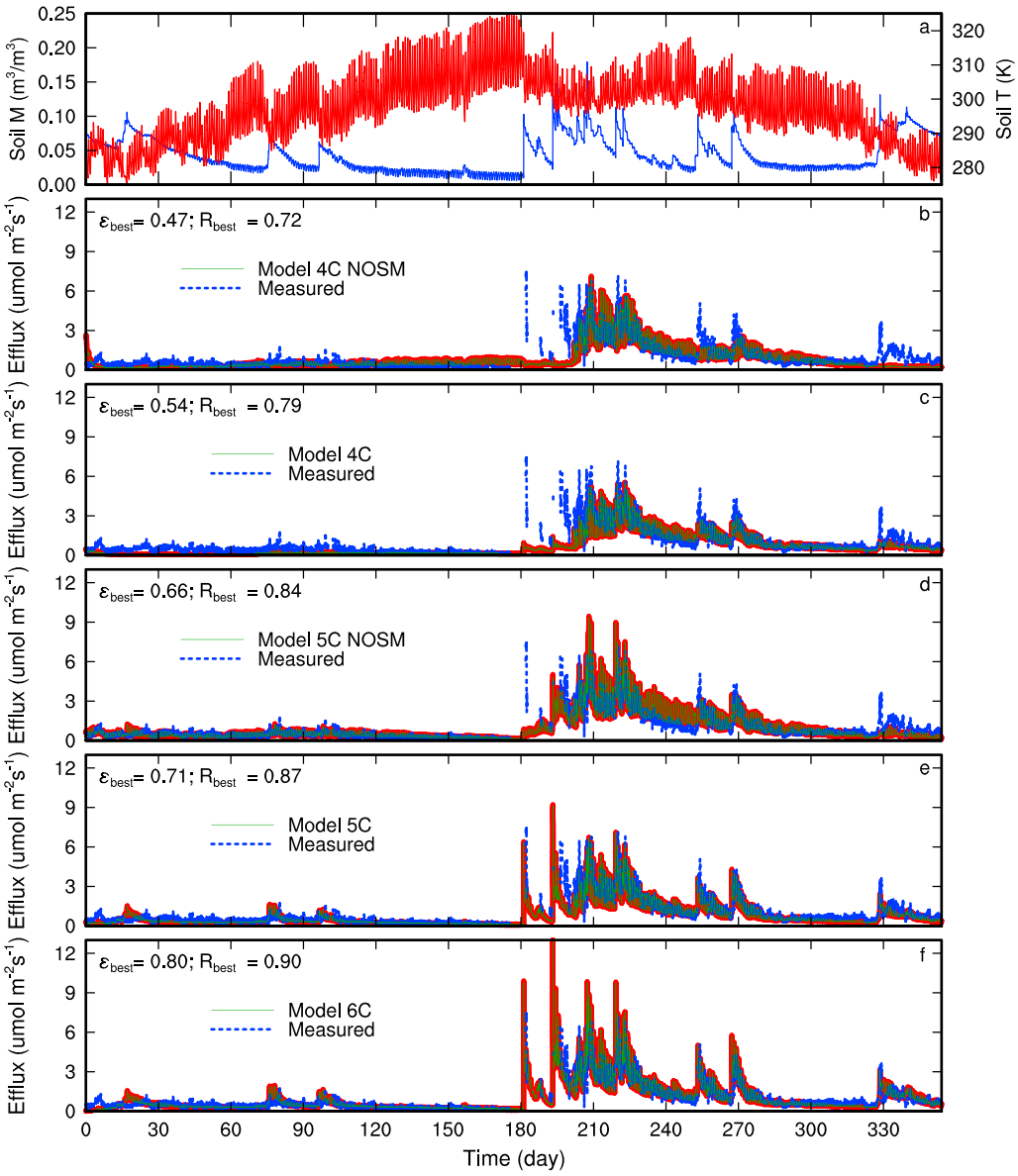

Figure 2. (a) Observed half-hourly volumetric soil moisture (in $m^3\ m^{-3}$) and temperature (in K) at 10 cm. Measured half-hourly CO_2 efflux at the soil surface (in $\mu mol\ m^{-2}\ s^{-1}$) compared with those modeled by the (b) 4C_NOSM, (c) 4C, (d) 5C_NOSM, (e) 5C, and (f) 6C models. The shaded area (in red) represents the 95% credible interval, while the green line is for the best realization. In the legends, ε_{best} stands for model efficiency and R_{best} for the correlation coefficient of the best realization.

3. Results Analyses

Driven by the observed soil moisture and temperature (Figure 2a), models 4C and 5C with soil moisture controls result in much lower ΔBIC and higher model probabilities than models 4C_NOSM and 5C_NOSM that are without soil moisture controls (Table 2 and Figure 2). With an additional DOC pool in the dry zone, models 5C and 5C_NOSM have lower ΔBIC and higher model probabilities than models 4C and 4C_NOSM, respectively. Model 6C with additional DOC and ENZ pools in the dry soil pores further improves the simulation with the lowest ΔBIC and highest model probability (Table 2). The model efficiency results (Table 2) indicate that model 6C has generally the highest model efficiency followed by model 5C and then model 4C, which is consistent with the ΔBIC and model probability results. This suggests that models with explicit moisture controls and with extra C pools are preferable.

©2014. American Geophysical Union. All Rights Reserved.

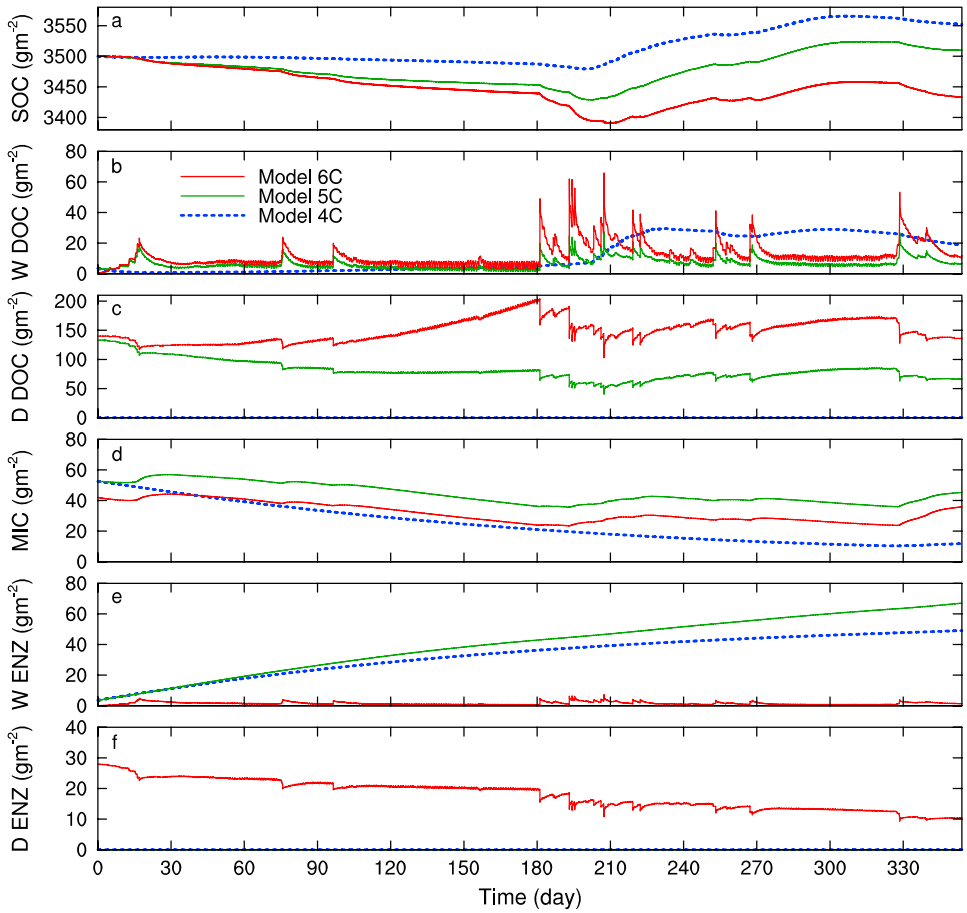

Figure 3. C storages of the best realizations by the 4C, 5C, and 6C models: (a) total SOC, (b) DOC in the wet zone, (c) degraded C in the dry zone, (d) microbial biomass, (e) enzymes in the wet zone, and (f) enzymes in the dry zone.

During the dry periods, the degraded C in models 5C and 6C accumulates in the dry pores (Figure 3c) since the degraded C is not accessible to microbes. In the wet pores, in response to the monsoon rainstorms, the degraded C immediately converts into DOC (Figure 3b), becoming readily available for microbial use. Since model 6C includes an extra SOC degradation process through catalysis of the enzymes in the dry pores (Figure 3f), which is assumed to function during dry conditions, model 6C results in a greater accumulation of degraded C in the dry pores (Figure 3c) and thus a larger volume of degraded C that is transitioned to DOC in the wet pores (Figure 3b). The cumulative CO_2 efflux for the entire modeling period modeled by models 4C, 5C, and 6C are 210, 237, and 293 g m^{-2}, about 30%, 22%, and 3% lower than the observed (302 g m^{-2}), respectively. This indicates that a proper representation of the Birch pulses may have long-term effects on the modeled soil C storage (Figure 3a) and changes in atmospheric CO_2 concentration.

4. Conclusions

Recent microbial enzyme-based models that incorporated the DAMM kinetics improved the representation of the temperature sensitivity of SOC decomposition, yet poorly capture dry-wet pulse dynamics. Our rigorous assessment of the five models developed in this study using techniques of model selection and model averaging suggests that models with additional C pools for accumulation of degraded C in the dry soil pores result in a higher probability of reproducing the observed Birch pulses. In response to rainstorms, labile C accumulated in the dry pores during dry periods becomes immediately accessible to microbes, providing a major mechanism to generate respiration pulses. Transition of labile C between the dry and wet soil pores helps maintain an amount of labile C in the dry pores (model 5C in Figure 3c) during dry periods (because it is not accessible to microbes). Including this mechanism, together with the soil moisture controls on the rates of SOC degradation and microbial uptake, improves the model's efficiency of simulating the

©2014. American Geophysical Union. All Rights Reserved.

Birch effect (model 5C in Figure 2). Assuming that enzymes in the dry soil pores facilitate SOC degradation during dry periods (model 6C) results in a greater accumulation of labile C in the dry pores (model 6C in Figure 3c) and thus further improves the model's efficiency (model 6C in Figure 2). However, revealing the actual mechanism inducing the greater accumulation in the dry pores still needs further experimental studies, because it may also attribute to many other mechanisms as summarized in *Moyano et al*. [2013]. Photodegradation of surface litter may be a pathway, but its effect is largely reduced through attenuation of ultraviolet radiation by the soil film formed through deposition of soil particles on the litter at this dryland site [*Barnes et al*., 2012]. With climate change, including an increase in variability of precipitation frequency and intensity, understanding and representing the Birch pulses will become an issue of global importance.

Acknowledgments

This work was partly supported by projects of NSF (EAR-1331408), DOE (DE-SC0006773), NSF (EF 1065790), the National Basic Research Program of China (grant 2011CB952002), National Natural Science Foundation of China (grant 41275090), Chinese Academy of Sciences Strategic Priority Program (grant No. XDA05090206), and DOE Early Career Award DE-SC0008272. The Santa Rita flux tower data (US-SRM) used in the paper are available online at the AmeriFlux website: http://ameriflux.ornl.gov. Additional soil CO_2 efflux data and the FORTRAN code for the five models are available online at http://b2science.org/earth/people/res/niu. We also thank the four anonymous reviewers for their constructive comments that help improve the quality of the paper.

The Editor thanks Steven Allison and one anonymous reviewer for their assistance in evaluating this paper.

References

Allison, S. D., M. D. Wallenstein, and M. A. Bradford (2010), Soil-carbon response to warming dependent on microbial physiology, *Nat. Geosci.*, *3*, 336–340.

Alster, C. J., D. P. German, Y. Lu, and S. D. Allison (2013), Microbial enzymatic responses to drought and to nitrogen addition in a southern California grassland, *Soil Biol. Biochem.*, *64*, 68–79.

Barnes, P. W., H. L. Throop, D. B. Hewins, M. L. Abbene, and S. R. Archer (2012), Soil coverage reduces photodegradation and promotes the development of soil-microbial films on dryland leaf litter, *Ecosystems*, *15*, 311–321, doi:10.1007/s10021-011-9511-1.

Barron-Gafford, G. A., R. L. Scott, G. D. Jenerette, and T. E. Huxman (2011), The relative controls of temperature, soil moisture, and plant functional group on soil CO_2 efflux at diel, seasonal, and annual scales, *J. Geophys. Res.*, *116*, G01023, doi:10.1029/2010JG001442.

Birch, H. F. (1958), The effect of soil drying on humus decomposition and nitrogen availability, *Plant and Soil*, *10*, 9–31.

Bradford, M. A., C. A. Davies, S. D. Frey, T. R. Maddox, J. M. Melillo, J. E. Mohan, J. F. Reynolds, K. K. Treseder, and M. D. Wallenstein (2008), Thermal adaptation of soil microbial respiration tolerated temperature, *Ecol. Lett.*, *11*, 1316–1327.

Davidson, E. A., and I. A. Janssens (2006), Temperature sensitivity of soil carbon decomposition and feedbacks to climate change, *Nature*, *440*, 165–173.

Davidson, E. A., S. Samanta, S. S. Caramori, and K. Savage (2012), The Dual Arrhenius and Michaelis-Menten kinetics model for decomposition of soil organic matter at hourly to seasonal time scales, *Global Change Biol.*, *18*, 371–384.

Frey, S. D., J. Lee, J. M. Melillo, and J. Six (2013), The temperature response of soil microbial efficiency and its feedback to climate, *Nat. Clim. Change*, *3*, 395–398.

Friedlingstein, P., et al. (2006), Climate-carbon cycle feedback analysis: Results from the C4MIP Model intercomparison, *J. Clim.*, *19*, 3337–3353.

Gelman, A., and D. B. Rubin (1992), Inference from iterative simulation using multiple sequences, *Stat. Sci.*, *7*(4), 457–472.

Jarvis, P. A., et al. (2007), Drying and wetting of Mediterranean soils stimulates decomposition and C dioxide emission: The "Birch effect", *Tree Physiol.*, *27*, 929–940.

Kass, R. E., and A. E. Raftery (1995), Bayes factors, *J. Am. Stat. Assoc.*, *90*(430), 773–795.

Laloy, E., and J. A. Vrugt (2012), High-dimensional posterior exploration of hydrologic models using multiple-try DREAM(ZS) and high-performance computing, *Water Resour. Res. 48*, W01526, doi:10.1029/2011WR010608.

Lawrence, C. R., J. C. Neff, and J. P. Schimel (2009), Does adding microbial mechanisms of decomposition improve soil organic matter models? A comparison of four models using data from a pulsed rewetting experiment, *Soil Biol. Biochem.*, *41*, 1923–1934.

Luo, Y. Q., S. Wan, D. Hui, and L. L. Wallace (2001), Acclimatization of soil respiration to warming in a tall grass prairie, *Nature*, *413*, 622–625.

Manzoni, S., P. Taylor, A. Richter, A. Porporato, and G. I. Agren (2012), Environmental and stoichiometric controls on microbial carbon-use efficiency in soils, *New Phytol.*, *196*, 79–91.

McClaran, M. P., J. Moore-Kucera, D. A. Martens, J. van Haren, and S. E. Marsh (2008), Soil carbon and nitrogen in relation to shrub size and death in a semi-arid grassland, *Geoderma*, *145*, 60–68.

Miller, A. E., J. P. Schimel, T. Meixner, J. O. Sickman, and J. M. Melack (2005), Episodic rewetting enhances carbon and nitrogen release from chaparral soils, *Soil Biol. Biochem.*, *37*, 2195–2204.

Moyano, F. E., S. Manzoni, and C. Chenu (2013), Responses of soil heterotrophic respiration to moisture availability: An exploration of processes and models, *Soil Biol. Biochem.*, *59*, 72–85.

Niu, G. Y., et al. (2011), The community Noah land surface model with multi-parameterization options (Noah-MP): 1. Model description and evaluation with local-scale measurements, *J. Geophys. Res.*, *116*, D12109, doi:10.1029/2010JD015139.

Reichstein, M., and C. Beer (2008), Soil respiration across scales: The importance of a model–data integration framework for data interpretation, *J. Plant Nutr. Soil Sci.*, *171*, 344–354.

Schimel, J. P., and M. N. Weintraub (2003), The implications of exoenzyme activity on microbial C and nitrogen limitation in soil: A theoretical model, *Soil Biol. Biochem.*, *35*, 549–563.

Schimel, J. P., T. C. Balser, and M. Wallenstein (2007), Microbial stress-response physiology and its implications for ecosystem function, *Ecology*, *88*, 1386–1394.

Schlesinger, W. H., and J. A. Andrews (2000), Soil respiration and the global carbon cycle, *Biogeochemistry*, *48*, 7–20.

Schmidt, M. W. I., et al. (2011), Persistence of soil organic matter as an ecosystem property, *Nature*, *478*, 49–56.

Scott, R. L., G. D. Jenerette, D. L. Potts, and T. E. Huxman (2009), Effects of seasonal drought on net carbon dioxide exchange from a woody plant encroached semiarid grassland, *J. Geophys. Res.*, *114*, G04004, doi:10.1029/2008JG000900.

Sinsabaugh, R. L., R. K. Antibus, and A. E. Linkins (1991), An enzymic approach to the analysis of microbial activity during plant litter decomposition, *Agr. Ecosyst. Environ.*, *34*, 43–54.

Skopp, J., M. Jawson, and J. Doran (1990), Steady-state aerobic microbial activity as a function of soil-water content, *Soil Sci. Soc. Am. J.*, *54*, 1619–1625.

Todd-Brown, K. E. O., J. T. Randerson, W. M. Post, F. M. Hoffman, C. Tarnocai, E. A. G. Schuur, and S. D. Allison (2013), Causes of variation in soil carbon predictions from CMIP5 Earth system models and comparison with observations, *Biogeosciences*, *10*, 1717–1736.

Wieder, W. R., G. B. Bonan, and S. D. Allison (2013), Global soil carbon predictions are improved by modeling microbial processes, *Nat. Clim. Change*, *3*, 909–912.

Ye, M., P. D. Meyer, and S. P. Neuman (2008), On model selection criteria in multimodel analysis, *Water Resour. Res.*, *44*, W03428, doi:10.1029/2008WR006803.

©2014. American Geophysical Union. All Rights Reserved.